Ind. J. Pharm. Edu. Res., 2027; 61:10.5530/ijper.20270174.
https://www.ijper.org

Original Article

Central Composite Design Based Optimization of Faropenem-Loaded Functionalized Carbon Nanotubes for Enhanced Antibacterial Activity

Vedanshu Malviya[1,*], Snehal Manekar[2], Ketakee Nichat[1], Pratiksha Makode[3]

[1]Department of Pharmaceutics, School of Pharmacy, GH Raisoni University, Amravati, Maharashtra, INDIA.
[2]Department of Pharmacognosy, Dr. Rajendra Gode Institute of Pharmacy, Amravati, Maharashtra, INDIA.
[3]Department of Pharmaceutical Chemistry, School of Pharmacy, GH Raisoni University, Amravati, Maharashtra, INDIA.

ABSTRACT

Background: More intelligent delivery of antimicrobials is required. The antibiotic Faropenem is a broad spectrum penem antibiotic, which is not very stable and has to be given several times a day. This study uses functionalized Multi-Walled Carbon Nanotubes (MWCNTs) as nanocarriers to improve the delivery of Faropenem a broad-spectrum antibiotic that typically suffers from poor stability and requires frequent daily dosing. Using the Central Composite Design (CCD) method, the researchers systematically optimized the formulation to enhance the drug's antibacterial effectiveness. **Materials and Methods:** Three factor CCD (CNT concentration, drug:CNT ratio, sonication time) was used for loading MWCNTs with Faropenem, and the carboxyl functionalized MWCNTs were loaded with Faropenem. The drug loading efficiency, particle size, zeta potential, *in vitro* release kinetics and antibacterial activity against *S. aureus* and *E. coli* were evaluated in 20 batches. Optimized formulation was further characterized by FTIR, DSC, XRD and stability studies. **Results:** Drug loading efficiency ranged from 45.8±2.0% to 86.4±1.3%, with the optimized batch (FCNT10) achieving 78.5±1.5% loading, 255.3±2.8 nm particle size, -43.42±1.3 mV zeta potential, and 82.9±1.4% yield. The formulation exhibited Korsmeyer Peppas kinetics with an anomalous transport (n=0.544±0.011) and resulted in the release of 67.5±1.5% of the drug after 24 hr. The zones of inhibition against *S. aureus* and *E. coli* were enhanced significantly (28.6±1.1 mm and 24.3±1.0 mm, respectively, vs. 18.4±0.9 mm and 16.2±0.8 mm, respectively, for pure faropenem). TEM revealed uniform drug adsorption along the intact nanotubes. No changes were observed in the formulation after 90 days of refrigeration (4°C). **Conclusion:** The optimized faropenem-loaded functionalized MWCNT formulation demonstrated enhanced antibacterial activity and sustained drug release under *in vitro* conditions. These findings suggest that functionalized carbon nanotubes represent a promising platform for controlled antibiotic delivery; however, further biocompatibility and *in vivo* investigations are required before clinical translation.

Keywords: Central Composite Design, Faropenem, Functionalized Multi-Walled Carbon Nanotubes, Response Surface Methodology, Sustained Antibacterial Release.

Correspondence:
Vedanshu Malviya
Department of Pharmaceutics, School of Pharmacy, GH Raisoni University, Amravati-444701, Maharashtra, INDIA.
Email: vedanshumlv56@gmail.com

Received: 28-05-2026;
Revised: 14-07-2026;
Accepted: 02-09-2026.

INTRODUCTION

Despite considerable progress in nanotechnology-assisted antimicrobial delivery, relatively few investigations have focused on the application of functionalized carbon nanotubes as carriers for β-lactam antibiotics, particularly faropenem.

Most previous studies involving carbon nanotubes have primarily explored the delivery of anticancer drugs, nucleic acids, antifungal agents, or model therapeutic compounds, whereas their application in enhancing the stability and sustained release of orally active penem antibiotics remains largely unexplored. Recent advances in antimicrobial nanomedicine have demonstrated that nanocarriers not only improve the physicochemical stability of antibiotics but also enhance bacterial targeting, prolong drug residence time, reduce premature degradation, and enable controlled drug release. These advantages are particularly valuable for β-lactam antibiotics, whose therapeutic efficacy is often compromised by instability and frequent dosing requirements. Consequently, nanotechnology-based delivery systems are increasingly being explored as promising tools to improve the therapeutic effectiveness of existing antibiotics rather than relying solely on the development of new antimicrobial agents.[1]

Functionalized carbon nanotubes possess unique structural characteristics that distinguish them from conventional nanocarriers. Their hollow tubular architecture, exceptionally

DOI: 10.5530/ijper.20270174

Copyright Information :
Copyright Author (s) 2027 Distributed under Creative Commons CC-BY 4.0

Publishing Partner : Manuscript Technomedia. [www.mstechnomedia.com]

high aspect ratio, and large specific surface area permit efficient loading of therapeutic molecules through π-π stacking, hydrophobic interactions, hydrogen bonding, and electrostatic adsorption. Surface functionalization with hydrophilic groups such as carboxyl (-COOH) significantly enhances aqueous dispersibility, minimizes aggregation, and improves compatibility with biological systems. These properties collectively enable higher drug-loading capacity, sustained release behaviour, and improved interaction with biological membranes, making functionalized MWCNTs promising candidates for antimicrobial drug delivery.[2]

Faropenem is a broad-spectrum oral penem antibiotic that demonstrates excellent activity against both Gram-positive and Gram-negative bacteria; however, its clinical effectiveness is limited by hydrolytic instability, relatively short biological half-life, and the requirement for repeated dosing. These limitations may reduce patient adherence and increase the risk of subtherapeutic antibiotic exposure, potentially contributing to antimicrobial resistance. Therefore, developing an optimized nanocarrier capable of protecting the drug, prolonging its release, and enhancing its antibacterial efficacy represents a promising strategy for improving faropenem therapy.[3] Encapsulation of faropenem within a functionalized nanocarrier may reduce premature degradation, improve drug stability during circulation, provide sustained release, and maintain therapeutic drug concentrations over prolonged periods. Such an approach has the potential to reduce dosing frequency while enhancing antibacterial efficacy, thereby improving patient compliance and supporting antimicrobial stewardship strategies.[4]

Among various nanocarriers, Carboxyl-Functionalized Multi-Walled Carbon Nanotubes (MWCNT-COOH) offer several advantages, including exceptionally high surface area, efficient non-covalent drug adsorption, tunable surface chemistry, enhanced aqueous dispersibility following functionalization, and the ability to facilitate sustained drug release. Furthermore, surface functionalization substantially improves the biocompatibility and colloidal stability of carbon nanotubes, making them attractive candidates for pharmaceutical drug delivery applications.[5]

Although functionalized carbon nanotubes have been extensively investigated for the delivery of anticancer drugs and selected antimicrobial agents, reports describing statistically optimized faropenem-loaded MWCNT formulations remain scarce. Moreover, the influence of formulation variables on drug loading efficiency, particle characteristics, release behaviour, and antibacterial performance has not been comprehensively investigated using a response surface methodology.[5]

Although they are promising, CNTs have not been translated clinically because of concerns about their cytotoxicity and inflammogenicity, mainly due to surface hydrophobicity, length and residual metal catalysts. Carboxyl functionalization, however, greatly reduces these toxic effects by improving dispersibility, decreasing protein corona formation and facilitating renal clearance of shorter fragments. We aim to achieve a balance between efficacy and an acceptable safety profile by using well characterized, highly purified MWCNT COOH (≥95% purity) and a systematic optimization approach.[6-8] Nevertheless, these proposed advantages of carboxyl functionalization do not establish the safety of the present formulation, and possible tissue persistence, cellular uptake, inflammatory responses and long-term accumulation of MWCNTs require dedicated biological investigation.

Although carboxyl functionalization and the high purity of the MWCNT-COOH may improve aqueous dispersibility and reduce some toxicity-related concerns, the present study did not include direct cytotoxicity, hemolysis/hemocompatibility, or *in vivo* toxicological evaluation. Therefore, the present findings demonstrate formulation performance and antibacterial potential but should not be interpreted as evidence of biological safety. Comprehensive *in vitro* and *in vivo* safety studies will be required before further translational consideration

The present work addresses this knowledge gap by employing a Central Composite Design (CCD) to systematically optimize three critical formulation variables MWCNT concentration, drug-to-carrier ratio, and sonication time with the objective of maximizing drug loading while achieving controlled release and improved antibacterial activity. The combination of nanotechnology-based drug delivery with statistical optimization provides a rational approach for developing reproducible formulations with enhanced pharmaceutical performance. Previous studies indicate that the biological response to MWCNTs is strongly dependent on their length, diameter, surface functionalization, purity, aggregation state and residual catalyst content; therefore, functionalization may modify but does not eliminate toxicity concerns.[9,10]

The present study systematically evaluates the combined influence of nanotube concentration, drug-to-carrier ratio, and sonication time on drug loading efficiency, particle characteristics, release kinetics, and antibacterial activity. This integrated experimental design provides a reproducible formulation strategy that may facilitate the future development of optimized carbon nanotube-based antibiotic delivery systems.

MATERIALS AND METHODS

The drug, Faropenem, was sourced from Yarrowchem Pvt. Ltd., Mumbai. The Multi-Walled Carbon Nanotubes Functionalized with Carboxyl Group (MWCNT-COOH) were purchased from Platonic Nanotech Jharkhand with a purity of more than 95%. The chitosan of medium molecular weight was obtained from Suvidhinath Laboratories, Gujarat. Tween 80 was purchased from Mumbai. In the study both analytical grade ethanol and distilled water were used. All other reagents and chemicals used were of analytical grade. Evaluation of cytotoxicity and *in vivo* safety was

beyond the scope of the present formulation development study and will be considered in subsequent investigations.

Methods

Standard Calibration Curve

To prepare a standard calibration curve using faropenem, an accurately weighed amount of the drug was dissolved in distilled water to make a stock solution of 100 µg/mL and then a set of standard calibration solutions were prepared by serial dilutions of the stock solution. From this, working concentrations between 2 and 12 µg/mL were created by serial dilution. The absorbance plots were scanned in the UV region (200-400nm) to determine λ_{max} (wavelength of maximum absorbance) which was 286nm. The absorbance of each dilution was then measured at this wavelength and distilled water was used as a blank.[11] The absorbance plots were analyzed in the UV range of 200-400 nm to find λ_{max}, which was identified at 286 nm. Distilled water served as the blank for initial calibration. A matrix-matched blank, made from the supernatant of unloaded MWCNT-COOH, confirmed minimal background absorbance at 286 nm (A<0.005), indicating that the CNT matrix does not interfere with drug quantification. A calibration curve was constructed using the concentration vs the absorbance value and the linearity was checked with the regression equation. This approach guarantees accurate quantification of the drug in further analysis.

Drug-Excipients Interaction Study

FTIR Study

In the case of Fourier Transform Infrared (FTIR) spectroscopy, we prepared a plain functionalized carbon nanotube (MWCNT-COOH), a physical mixture of both and the final optimized lyophilized formulation. All samples were gently ground under hydraulic pressure with spectroscopic grade potassium bromide to produce a clear pellet. The pellet has been scanned between 4000 and 400 cm^{-1} with the resolution of 4 cm^{-1}. The resulting spectra were compared to see whether there were significant shifts, disappearance or broadening of characteristic peaks of faropenem, such as β lactam carbonyl, amide bands.[12] Absence of major changes of the drug's functional group bands proved the chemical compatibility between faropenem and the carrier, thus confirming the integrity of the drug in the formulation process.

DSC Study

To check if there is any interaction between faropenem and the functionalized carbon nanotubes, differential scanning calorimetry was conducted. A sealed aluminium pan was used to accurately weigh each sample (≈3-5 mg) for each sample (faropenem, MWCNT-COOH, physical mixture, lyophilized formulation). Blank pan was used as a control. The scan was done in a nitrogen flow (50 mL/min) and the temperature range was between 30-300°C, with a constant ramp-up of 10°C/min. The melting endotherm, peak temperature and enthalpy of the fusion of faropenem were analyzed in the thermograms.[13] Compatibility was assessed based on both chemical and physical compatibility criteria. Chemical compatibility was indicated by the absence of new peaks or significant shifts in existing peaks that would suggest chemical reactions between drug and carrier. Physical compatibility was evaluated by the preservation of the drug's melting endotherm with peak temperature shift of less than 2°C and maintenance of at least 50% of the drug's enthalpy of fusion, indicating that the drug retains its crystalline character without complete amorphization or degradation.

Crystallinity Evaluation

To evaluate the crystallinity of the loaded faropenem, the functionalized carbon nanotubes were placed in an X-ray diffractometer. The finely powdered samples of pure faropenem, plain MWCNT-COOH, physical mixture and the optimized formulation were loaded into a quartz sample holder. The diffractometer was used at 40 kV and 30 mA with Cu Kα radiation (λ=1.5406 Å). Scans were taken within a range of 2θ (5-50°) with a step size of 0.02° and a scan rate of 2°/min. The diffractograms obtained were compared for characteristic sharp peaks of Faropenem.[14] The partial amorphization was suggested by a decrease in the intensity of the peaks and/or the broadening of the peaks, whereas complete disappearance of the drug peaks implied the dispersion of the drug molecules at the molecular level or amorphization in the CNT matrix.

Formulation of the MWCNT's

A Central Composite Design (CCD) method was used to optimize the formulation components of functionalized Carbon Nanotubes (CNTs) (Table 1) systematically. In brief, Carboxyl-functionalized multi-walled carbon nanotubes (MWCNT-COOH) were accurately weighed (5-15 mg) and suspended in distilled water containing 0.5% v/v Tween 80 (to aid dispersion and prevent aggregation) and 0.1% w/v chitosan (as a stabilizer to prevent nanotube aggregation during sonication). The mixture was probe-sonicated for 5-15 min to achieve uniform dispersion. Faropenem (200 mg) was then added at drug:CNT ratios of 1:0.5, 1:1, or 1:1.5. The final formulations were centrifuged, and the pellet was lyophilized. All 20 CCD batches received the same concentrations of chitosan and Tween 80, which were included as auxiliary excipients and not as independent variables.

To ensure a good dispersion of the mixture, the aggregation is minimized, and the amount of drug loaded onto the nanotube surface is maximized, the mixture was probe sonicated for controlled periods of 5, 10, and 15 min. Strong interaction between the drug molecules and the functionalized CNT surface was promoted by sonication, thus enhancing the adsorption efficiency. The formulation was sonicated for equilibration, followed by centrifugation to eliminate unbound drug to give a stable CNT-drug complex.[15-17] The effect of these parameters

on drug loading efficiency, particle size and drug release was investigated by preparing various experimental batches that differed in the ratios of CNTs to drugs, varying the sonication time, and varying the ratio of CNTs to drugs.

Evaluation Parameters

Drug Loading Efficiency (%)

The batches of CNT were prepared as Faropenem complex and each formulation was subjected to three successive centrifugation-wash cycles at 4°C and 15,000 rpm for 30 min per cycle. Following each centrifugation step, the supernatant was carefully removed, and the pellet was resuspended in 5 mL of fresh distilled water before the next cycle. The supernatants from all three cycles were pooled, diluted appropriately with distilled water, and analyzed for unbound drug content by UV-vis spectrophotometry at 286 nm using the pre-validated calibration curve. Absence of detectable drug in the third wash supernatant confirmed complete removal of unbound drug.[18] The efficiency of the loading of the drug was calculated as:

$$\frac{\text{Initial drug} - \text{Unbound drug}}{\text{Initial drug}} \times 100\%$$

The 20 experimental batches were tested three times. The supernatant from the first centrifugation was re-centrifuged and re-analysed to confirm complete removal of unbound drug. No detectable drug was found in the second supernatant, confirming that all measured unbound drug was accurately accounted for in the loading calculation.

The loading efficiency of various levels of the factors (CNT concentration, drug to CNT ratio, sonication time) was compared using a One Way Analysis of Variance (ANOVA). A p value of <0.05 was regarded as statistically significant and it was found that the formulation variables had significant effect on the drug loading. The statistical approach proved the reliability of the optimization process.

Particle Size (nm)

The sizes of the particles were determined by dynamic light scattering using a Malvern Zetasizer Nano ZS (Malvern Instruments, UK) at 25°C with a detection angle of 173°. Each CCD batch lyophilized formulation was redispersed in distilled water at 1 mg/mL and gently vortexed. A volume of about 1 mL of the dispersion was placed in a disposable cuvette of polystyrene. All samples were triplicated and the average hydrodynamic diameter obtained (nm).[19] To analyze the effect of the independent variables (CNT concentration, drug:CNT ratio, sonication time) on particle size, two way and three-way ANOVA were performed. This enabled the main effect and interaction effects of the factors to be determined. ANOVA evaluation revealed that the particle size reduction was significantly different between the different formulation conditions, i.e., sonication time and CNT concentration, to guide optimal formulation conditions.

Polydispersity Index (PDI)

The PDI was measured directly at the same measurement of particle size used for the dynamic light scattering, which is a measure of the width of the particle size distribution. The PDI value was automatically calculated by the instrument software using the cumulants analysis. A PDI of <0.3 suggested a narrow, homogeneous distribution, a PDI of >0.5 indicated broad distribution.[20] Three measurements were taken for each of the 20 batch formulations and the average PDI is reported. A multifactor ANOVA was performed to determine if formulation variables had a statistically significant effect on PDI

Zeta Potential (mV)

The same Zetasizer instrument was used to measure the zeta potential by laser Doppler electrophoresis. For the correct scattering intensity, the formulation was diluted 1:100 with distilled water. The diluted sample was introduced to the capillary cell without any air bubbles in the sample. An electric field was applied to the instrument and electrophoretic mobility was then converted to zeta potential.[21] All CCD batches were measured three times at 25°C. One way ANOVA was used to test the differences in zeta potential among the different CNT concentrations (5, 10, 15 mg). *post hoc* Tukey's tests further employed to find specific pair differences.

Percentage Yield

The 20 CCD formulation batches were freeze dried and the percentage yield was determined gravimetrically. The mass of the used solids (faropenem, functionalized CNTs and chitosan/Tween 80) was measured. After preparation, centrifugation and lyophilization, the final dried powder was carefully weighed.[22] The percentage yield was calculated as follows:

$$\%\ \text{Yield} = \frac{\text{Actual weight of recovered formulation}}{\text{Theoretical total weight of all components}} \times 100$$

A three-factor ANOVA (CNT concentration, drug:CNT ratio, sonication time) was used to assess the significance of the formulation variables on the yield.

In vitro Drug Release Study

The *in vitro* release performance of the optimized CCD formulations was evaluated using a dialysis bag diffusion setup. Specifically, freeze-dried powder equivalent to 10 mg of faropenem was introduced into pre-soaked dialysis membranes (MWCO: 12-14 kDa), which were then hermetically sealed. Each bag was submerged in 900 mL of phosphate-buffered saline (PBS, pH 7.4) to simulate physiological conditions within a USP basket-type dissolution apparatus operating at 37±0.5°C and 100 rpm. The saturation solubility of faropenem in PBS (pH 7.4) at 37°C was determined to be 2.8±0.3 mg/mL. The maximum drug concentration in the release medium (10 mg/900 mL=0.011 mg/mL) was well below 10% of the saturation solubility (0.28 mg/

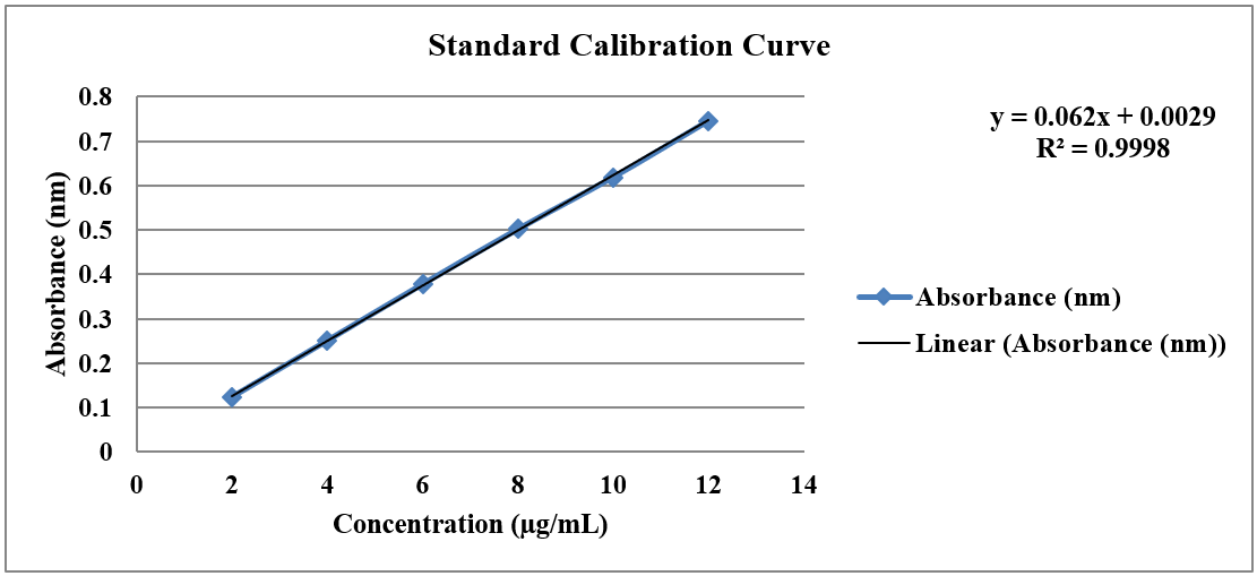
mL), thereby maintaining perfect sink conditions throughout the experiment. At designated time points (0.5, 1, 2, 4, 6, 8, 12, and 24 hr), 2 mL aliquots were withdrawn from the release medium and replaced with an equal volume of fresh PBS to maintain constant volume. Drug quantification in the collected samples was carried out using UV-vis spectrophotometry at 286 nm.[23,24] Finally, the resulting cumulative release data from the various batches were subjected to repeated measures ANOVA, with time treated as the intra-subject variable and formulation type as the inter-subject variable.

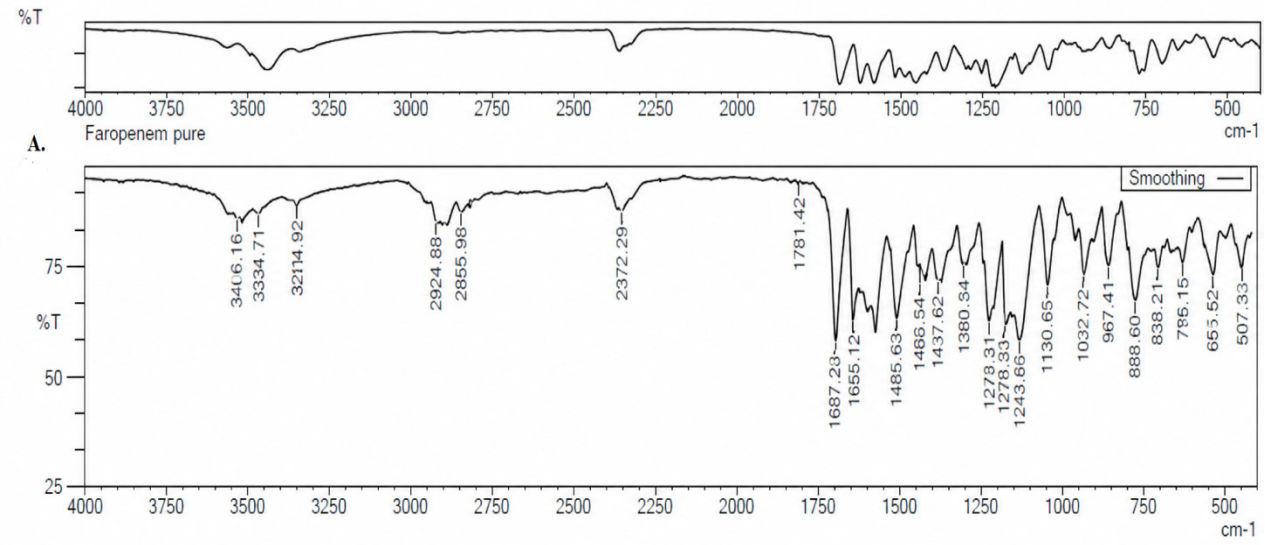
Drug Release Kinetics

The regression analysis for the cumulative percentage of drug released data from each batch of CCD were fitted to Zero order, 1st order, Higuchi, and Korsmeyer Peppas model. The model with the highest Coefficient of Determination (R^2) was chosen as the best fit model. The release mechanism was interpreted based on the cylindrical geometry of MWCNTs (as confirmed by TEM imaging), where the release exponent (n) from the Korsmeyer Peppas equation indicates Fickian diffusion (n=0.45), anomalous transport (0.45<n<1.0), or Case II transport (n=1.0). It is acknowledged that the formulation exhibits some polydispersity, which may result in a distribution of release exponents rather than a single value. The reported n value represents the average behavior of the population.[25] Comparisons of kinetic parameters of the different formulation variables were done by multivariate ANOVA (MANOVA) using drug:CNT ratio and sonication time as independent variables and release rate constants (k) as dependent variables.

Antibacterial Activity

The Agar well diffusion method was used to check the antibacterial activity against*Staphylococcus aureus* (gram positive) and*Escherichia coli* (gram negative). The drug content in the optimized CNT formulation was confirmed by UV-vis spectrophotometry at 286 nm prior to antibacterial testing. A





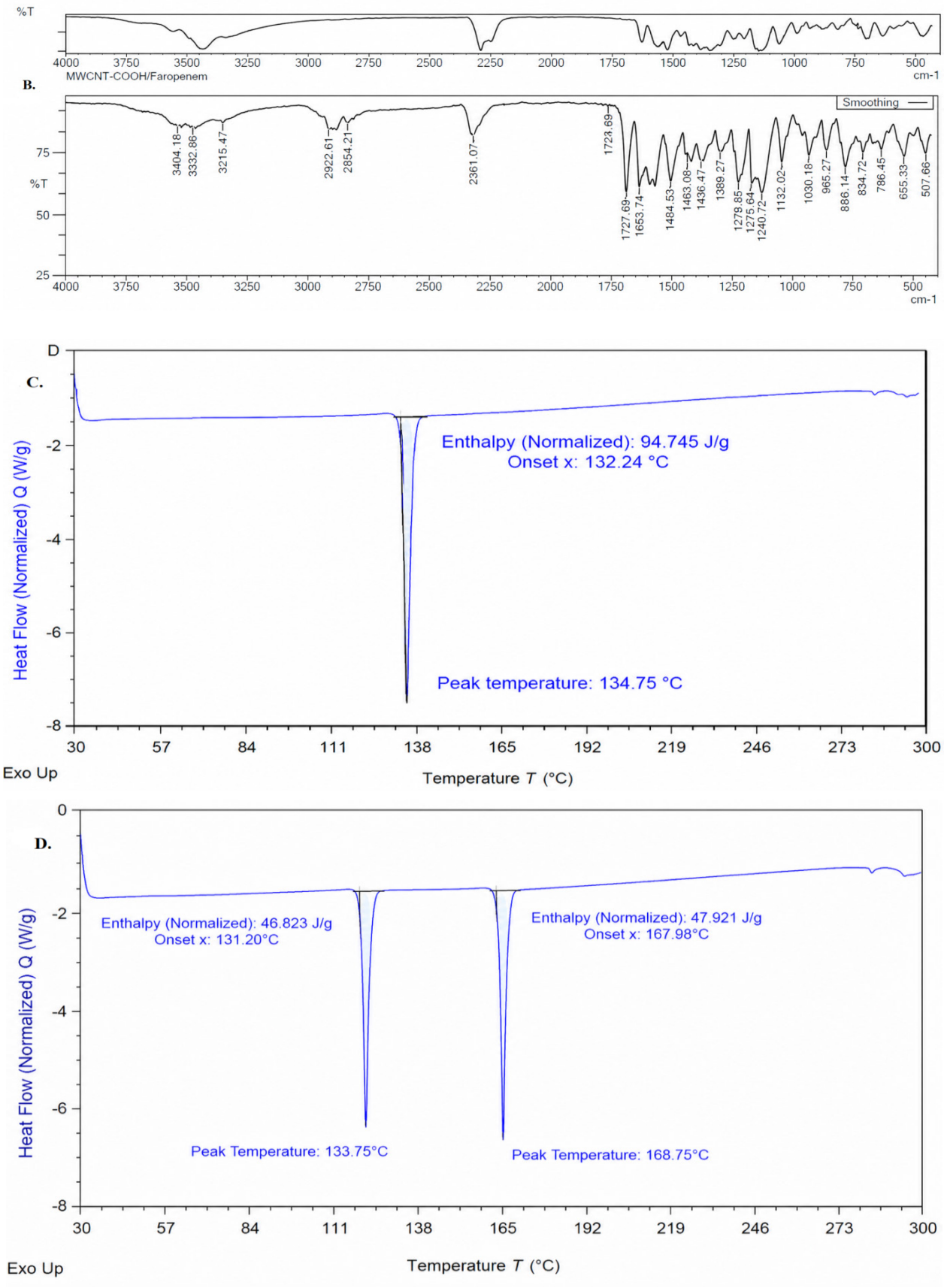


Figure 1: FTIR of Faropenem (A), FTIR of Optimized Formulation (B), DSC of Faropenem (C) and DSC of Optimized Formulation (D).

Table 1: Formulation Variables and Chart of the Multi-Walled CNTs

Batch	CNT Concentration (mg)	Drug:CNT ratio	Sonication Time (min)	Drug Loading Efficiency (%)	Particle Size (nm)	% Drug Release
FCNT1	-1 (5)	-1 (1:0.5)	1 (15)	52.3±1.8	312.5±4.2	91.2±2.1
FCNT 2	-1 (5)	1 (1:1.5)	1 (15)	68.7±2.1	298.4±3.9	85.6±1.9
FCNT 3	1 (15)	-1 (1:0.5)	1 (15)	81.2±1.5	265.8±3.5	68.4±1.7
FCNT 4	1(15)	1 (1:1.5)	1 (15)	86.4±1.3	248.9±3.1	58.2±1.5
FCNT 5	0 (10)	0 (1:1)	0 (10)	77.9±1.6	258.6±3.3	70.3±1.6
FCNT 6	0 (10)	1 (1:1.5)	0 (10)	82.5±1.4	251.2±3.0	63.7±1.5
FCNT 7	1(15)	1 (1:1.5)	-1 (5)	70.3±1.9	276.4±3.7	75.8±1.8
FCNT 8	1 (15)	0 (1:1)	0 (10)	83.6±1.5	253.7±3.2	66.9±1.6
FCNT 9	-1 (5)	-1 (1:0.5)	-1 (5)	45.8±2.0	338.2±4.5	96.5±2.3
FCNT 10	0 (10)	0 (1:1)	0 (10)	78.5±1.5	255.3±2.8	67.5±1.5
FCNT 11	0 (10)	-1 (1:0.5)	0 (10)	69.4±1.7	264.1±3.4	78.4±1.8
FCNT 12	-1 (5)	1 (1:1.5)	-1 (5)	58.2±1.9	305.7±4.0	88.3±2.0
FCNT 13	1 (15)	-1 (1:0.5)	-1 (5)	74.6±1.7	288.3±3.8	79.2±1.9
FCNT 14	0 (10)	0 (1:1)	0 (10)	78.2±1.6	256.1±3.1	69.1±1.6
FCNT 15	0 (10)	0 (1:1)	-1 (5)	71.8±1.8	272.5±3.6	80.6±1.9
FCNT 16	0 (10)	0 (1:1)	0 (10)	78.8±1.4	254.8±2.9	68.8±1.5
FCNT 17	0 (10)	0 (1:1)	0 (10)	77.5±1.7	256.9±3.2	69.5±1.6
FCNT 18	0 (10)	0 (1:1)	1 (15)	80.1±1.5	249.6±3.0	60.4±1.4
FCNT 19	-1 (5)	0 (1:1)	0 (10)	63.5±1.8	289.7±3.8	82.3±1.9
FCNT 20	0 (10)	0 (1:1)	0 (10)	78.3±1.6	255.9±3.0	68.2±1.5

Values are mean±SD (n=3).

known amount of the lyophilized formulation was dissolved in distilled water, centrifuged to remove the CNT matrix, and the supernatant analyzed using the pre-validated calibration curve. The experimentally determined drug content (78.5±1.5%) was used to prepare an equivalent pure faropenem solution (50 µL containing 10 µg of faropenem) to enable a direct comparison of antibacterial potency. Bacterial cultures (0.5 McFarland) were freshly swabbed onto Mueller Hinton agars. Plates were incubated for 24 hr at 37°C. Three replicates were performed for each zone of inhibition in millimetres.[26,27] A two-way ANOVA was used to compare the influence of formulation type (pure drug vs. CNT formulation) and bacterial strain on the zone diameter. Optimized formulation was compared to pure faropenem using *post hoc* tests to establish superiority.

Morphology (TEM)

The diluted formulation was deposited on a carbon coated copper grid for Transmission Electron Microscopy (TEM), which was then negatively stained with 1% phosphotungstic acid. The grid was air dried and then observed using TEM at 100 kV. TEM images were taken at to obtain the surface morphology and the structure of the nanotube.[28]

Stability Study

The optimized formulation was stored in sealed glass vials under two conditions: refrigerated (4°C±2°C), room temperature (25°C±2°C/60%±5% RH and accelerated (40°C± 2°C/ 75%±5% RH) for 3 months. Sample was taken at 0, 30, 60 and 90 days, and evaluated for particle size, PDI, zeta potential, drug loading efficiency and *in vitro* drug release. Any visual changes were noted. Faropenem degradation was assessed by measuring using UV Vis spectrophotometry.[29-31] A two way repeated measures ANOVA was performed with storage condition and time being the factors.

Statistical Optimization

Each experiment was replicated three times and the results are presented as mean±SD. Central Composite Design (CCD) and quadratic regression models were used to guide the process of formulation optimisation. As appropriate, one way, two way and three way analysis of variance (ANOVA) were used to determine the effects of independent variables. *In vitro* release and stability data were analyzed by repeated measures ANOVA (time as within subject factor and formulation/storage condition as between subject factor). MANOVA was used to test multivariate effects on release kinetic parameters. Tukey's or Bonferroni's test were

used to perform *post hoc* pairwise comparisons. All tests were considered statistically significant with p values <0.05.

RESULTS

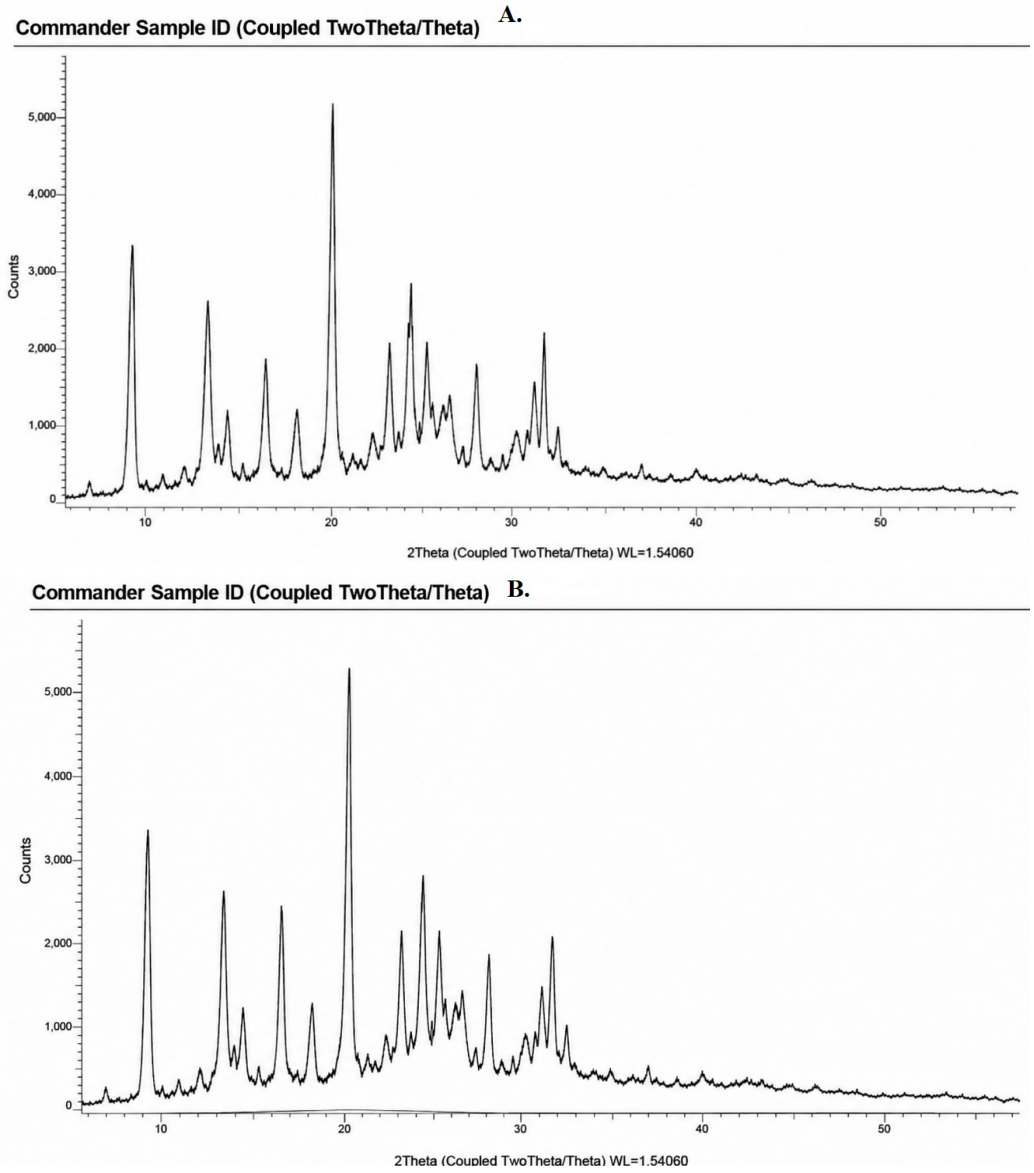
Standard Calibration Curve

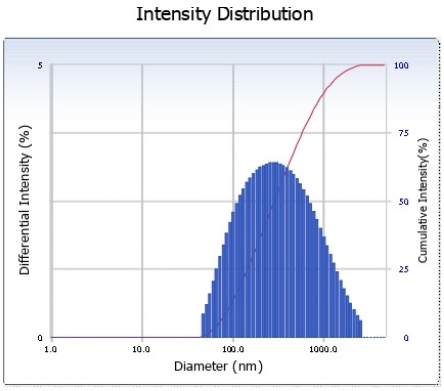
The calibration curve for faropenem was prepared by plotting the absorbance against the concentration (2-12 µg/mL). The data displayed in Figure 1 show a high degree of linearity (R^2=0.999) and the regression equation was y=0.062x±0.002. The high correlation obtained indicates the validity of Beer Lambert's law over the range of concentrations tested and suggests the method is reliable and appropriate for routine drug quantification in loading, release and stability studies.

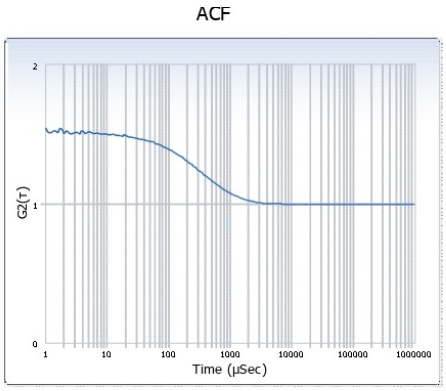
Drug-Excipients Interaction Study

The FTIR spectra of pure faropenem and optimized formulation of faropenem loaded MWCNT-COOH are shown in Figure 1. All major characteristic peaks of the pure drug were seen in the loaded formulation, showing no significant changes in structure. For the pure drugs, a wide O-H stretching band was observed at 3400 - 3300 cm^{-1} shifting slightly to its broader side after loading. The stretching vibrations of the C-H bonds were seen in the range 2920-2850 cm^{-1}, which is the region of aliphatic C-H stretching. Both spectra showed a strong absorption band at 1725-1780 cm^{-1}, which corresponds to the stretching of the C=O of the β-lactam and carboxylic groups, but small shifts (~2-3 cm^{-1}) were observed upon loading. The bands at 1650-1500 cm^{-1} (associated with C=C and amide vibrations) and peaks at 1300-1000 cm^{-1} (assigned to C-O and C-N stretches) were always present. The spectra of the fingerprint region, below 1000 cm^{-1}, showed little difference with no additional peaks appearing in the formulation spectra.

The DSC thermogram of pure faropenem shows a sharp melting endotherm at approximately 134.75°C, with an enthalpy of







Distribution Results (Contin)

Peak	Diameter (nm)	Std. Dev.
1	484.4	476.5
2	0.0	0.0
3	0.0	0.0
4	0.0	0.0
5	0.0	0.0
Average	484.4	476.5

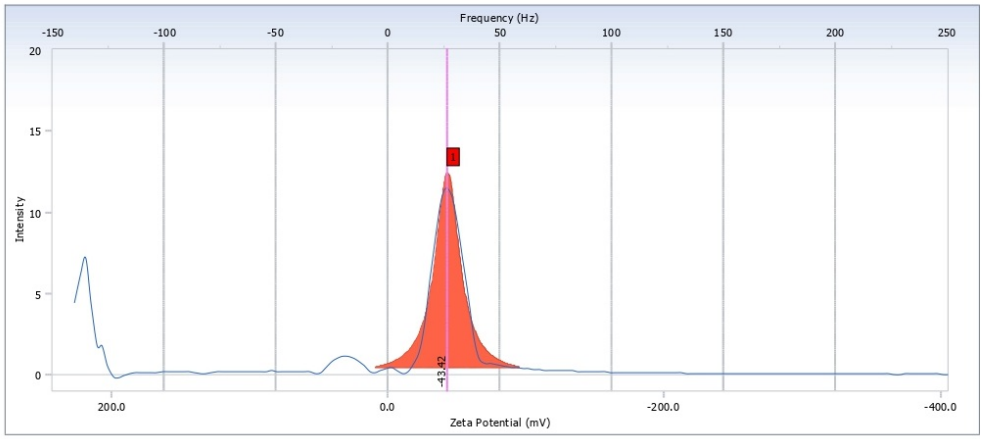
Residual : 2.720e-003 (O.K)

Cumulants Results

Diameter	(d)	: 255.3	(nm)
Polydispersity Index	(P.I.)	: 0.286	
Diffusion Const.	(D)	: 1.927e-008	(cm²/sec)

Measurement Condition

Temperature	: 25.0	(°C)
Diluent Name	: WATER	
Refractive Index	: 1.3328	
Viscosity	: 0.8878	(cP)
Scattering Intensity	: 32610	(cps)
Attenuator 1	: 6.52	(%)



Measurement Results

Zeta Potential	: -43.42	(mV)	Doppler shift	: 26.83	(Hz)
Mobility	: -3.386e-004	(cm²/Vs)	Base Frequency	: 121.7	(Hz)
Conductivity	: 0.0497	(mS/cm)	Conversion Equation	: Smoluchowski	

Zeta Potential of Cell

Upper Surface	: -40.20	(mV)
Lower Surface	: -43.42	(mV)

Cell Condition

Cell Type	: Flow Cell	
Avg. Electric Field	: -16.51	(V/cm)
Avg. Current	: -0.04	(mA)

Diluent Properties

Diluent Name	: WATER	
Temperature	: 25.0	(°C)
Refractive Index	: 1.3328	
Viscosity	: 0.8878	(cP)
Dielectric Constant	: 78.3	

Figure 2: XRD of Pure Drug (A), XRD of Optimized Formulation (B), Particle Size, Polydispersity Index, Zeta Potential of Optimized Formulation.

about 94.74 J/g, confirming its crystalline nature. In the loaded formulation, the melting peak shifts to 133.75°C with reduced enthalpy (46.82 J/g), indicating some interaction and lower crystallinity due to adsorption. A second peak at ~168.75°C is attributed to the MWCNT COOH matrix. The decrease in melting enthalpy suggests partial amorphization of faropenem within the CNT matrix, indicating significant molecular dispersion while some drug remains crystalline, likely adsorbed on the nanotube

Table 2: Results of Evaluation Parameters for All CCD Batches.

Batch No.	PDI	Zeta Potential (mV)	Percentage Yield (%)
FCNT1	0.412±0.021	-28.6±1.1	71.2±1.6
FCNT 2	0.356±0.018	-32.1±1.3	74.5±1.8
FCNT 3	0.298±0.015	-41.2±1.5	84.6±1.5
FCNT 4	0.272±0.012	-45.7±1.6	86.1±1.3
FCNT 5	0.291±0.014	-42.9±1.4	80.3±1.4
FCNT 6	0.278±0.013	-44.5±1.5	82.7±1.5
FCNT 7	0.322±0.016	-39.8±1.4	76.8±1.7
FCNT 8	0.283±0.013	-43.8±1.5	83.2±1.4
FCNT 9	0.478±0.024	-24.3±1.0	65.4±2.1
FCNT 10	0.286±0.012	-43.42±1.3	82.9±1.4
FCNT 11	0.308±0.015	-39.5±1.4	78.5±1.6
FCNT 12	0.385±0.019	-30.4±1.2	70.8±1.9
FCNT 13	0.335±0.017	-36.7±1.3	79.1±1.7
FCNT 14	0.288±0.013	-43.1±1.4	81.5±1.5
FCNT 15	0.315±0.016	-40.2±1.4	75.2±1.8
FCNT 16	0.284±0.011	-43.5±1.3	82.1±1.4
FCNT 17	0.289±0.014	-42.8±1.4	80.9±1.6
FCNT 18	0.275±0.012	-45.1±1.5	84.3±1.3
FCNT 19	0.348±0.017	-34.2±1.2	73.6±1.8
FCNT 20	0.287±0.013	-43.3±1.3	81.7±1.5

Values are mean±SD (n=3).

Table 3: Antibacterial Activity - Zone of Inhibition (mm).

Sample	*Staphylococcus aureus* (mm)	*Escherichia coli* (mm)
Pure Faropenem (50 µL, equivalent conc.)	18.4±0.9	16.2±0.8
Plain CNTs	9.2±0.6	8.5±0.5
Optimized Formulation (FCNT 10)	28.6±1.1	24.3±1.0

Values are mean±SD (n=3).

surface. With around 50% drug by weight, the theoretical enthalpy for the drug fraction is about 47.37 J/g, closely matching the observed value, which indicates that the drug's crystalline structure largely persists despite a slight reduction due to partial amorphization during adsorption, consistent with hydrogen bonding and π-π interactions.

Crystallinity Study

The X-ray diffraction (XRD) pattern of pure faropenem showed several sharp, intense diffraction peaks at the values of 2θ ~ 10°, 15°, 18°, 20° and 22°, which suggest that the faropenem crystals are highly crystalline and have a well-ordered lattice structure. For the MWCNT COOH loaded faropenem, most of these characteristic peaks were seen with slight shifts of ~2° (e.g., to ~12°, ~17°, and ~24°), indicating successful incorporation of the drug. A minor decrease in the peak intensity was seen along with a minor broadening, indicating some loss of crystallinity due to interaction with the carrier. The wide background signal of MWCNT COOH coincided with drug peaks, which is helpful for the formation of a composite system as shown in Figure 2. The preservation of characteristic faropenem peaks with reduced intensity confirms that the drug retains its crystalline structure in the formulation, albeit with partial amorphization as suggested by peak broadening. This partial amorphization is favorable for dissolution as it enhances the apparent solubility of the poorly soluble drug while maintaining sufficient crystallinity for stability.

Drug Loading Efficiency (%)

The efficiency of drug loading varied between 45.8±2.0% (batch FCNT9, low CNT, low drug:CNT ratio, low sonication) and 86.4±1.3% (batch FCNT4, high CNT, high ratio, high sonication) for the 20 batches in the central composite design (Table). The formulation (batch FCNT10) that has been optimized gave a loading efficiency of 78.5±1.5%, which was near to the CCD predicted value of 79.2%. A significant difference was observed for all three variables (one way ANOVA p<0.05) with the highest effect being observed when the concentration of CNT was compared (F=28.4, p=0.003). An increase in the CNT mass and the sonication time improved drug adsorption as did an increase

in the drug:CNT ratio (1:1.5) because of increased availability of the drug.

Particle Size (nm) and Polydispersity Index (PDI)

Particle sizes ranged from 248.9±3.1 nm (batch 4) to 338.2±4.5 nm (batch FCNT9). The optimized formulation (FCNT10) yielded the mean particle size of 255.3±2.8 nm which was found to be in a good agreement with the mean value predicted from the optimization of the formulation (254.8 nm) (Table and Figure 2). ANOVA revealed that the sonication time was the most significant factor (F=34.2, $p<0.001$), while the concentration of CNT had a significant effect (F=12.7, $p=0.012$). Increasing the CNT content (15 mg) and the sonication time (15 min) resulted in more compact complexes and reduced size of the aggregates, respectively. There was also a significant interaction between drug:CNT ratio and sonication ($p=0.027$).

PDI values for the different batches ranged from 0.272±0.012 (FCNT4) to 0.478±0.024 (FCNT9); the optimized formulation had a PDI value of 0.286±0.012, which is significantly less than the 0.3 value corresponding to a homogeneous dispersion (Table 2 and Figure 2). The ANOVA showed that the ratio of the dose of the drug to the CNT significantly affected PDI (F=8.9, $p=0.028$) and lower PDI was achieved when the dose of the drug was increased relative to the CNT, which is attributed to the good surface coverage.

Zeta Potential (mV)

Zeta potential values varied from -24.3±1.0 mV (FCNT9) to -45.7 1.6 mV (FCNT4) (Table and Figure 2). Optimized formulation showed good colloidal stability with a zeta potential of -43.42±1.3 mV. One way ANOVA revealed significant differences between the groups of CNT concentrations (F=11.3, $p=0.006$). The *post hoc* tests showed that the zeta potential of the batches containing 15 mg CNT was significantly more negative (mean -42.5 mV) than the batches containing 5 mg CNT (mean -29.1 mV, $p<0.01$).

Percentage Yield

Percentage yield across batches ranged from 65.4±2.1% (FCNT9) to 86.1±1.3% (FCNT4). In the optimized formulation (FCNT10), the yield was 82.9±1.4%, which was the same as predicted (83.5%) which can be seen in Table . Three factor ANOVA indicated that the CNT concentration significantly affected (F=9.6, $p=0.015$) the interaction effect of the CNT concentration and drug:CNT ratio was also significant ($p=0.041$). Drug adsorption was incomplete and loss during centrifugation was higher in batches with low CNT (5 mg), and they were therefore associated with lower yields.

In vitro Drug Release Profiles

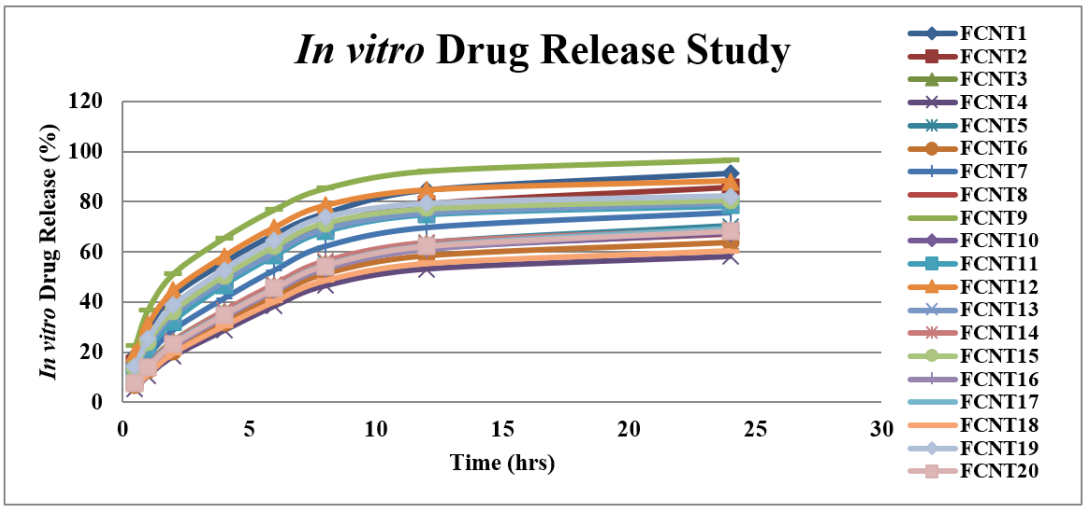
The outcome of the *in vitro* drug release profiles in Table and Figure 3 were found to be inconsistent with each other between different batches. The drug:CNT ratio (1:0.5) and low concentration of CNT (5 mg) and sonication (5 min) in the batch - such as FCNT9 - produced a very rapid burst release (96.5% at 24 hr). However, batches containing high CNT (15 mg) and high ratio (1:1.5) and long sonication (15 min) - i.e. FCNT4 and FCNT18 - exhibited sustained release (58-60% at 24 hr). The optimized formulation (FCNT10) showed a release of 67.5±1.5% at 24 hr as compared to 68.2% predicted by CCD. Repeated measures ANOVA revealed a significant effect of time (F=162.8, $p<0.001$), formulation type (F=31.4, $p<0.001$), and a significant time × formulation interaction (F=14.7, $p=0.006$).

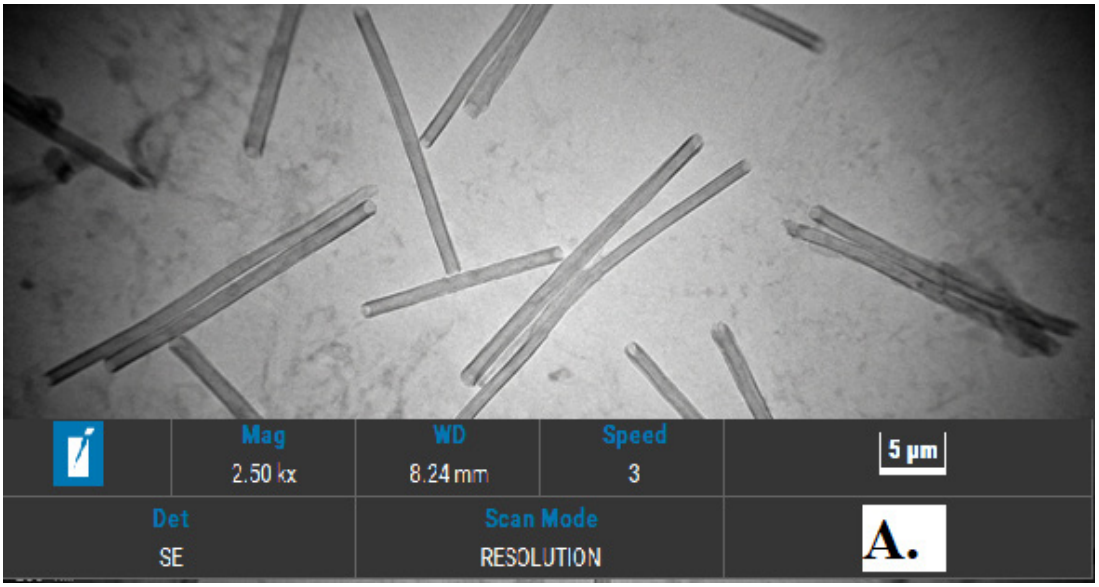
Drug Release Kinetics

Zero order, first order, Higuchi and Korsmeyer Peppas models were used for release kinetics. The majority of batches took place either in Higuchi (Fickian diffusion) or Korsmeyer Peppas (anomalous transport) kinetic regime. The optimized formulation (FCNT10) fit the Korsmeyer Peppas model (R^2=0.992±0.003) best and the release exponent (n) was 0.544±0.011, which is the number for anomalous (non Fickian) transport, comprising the interplay between diffusional release and polymer chain relaxation was also examined. MANOVA, with the Higuchi

Table 4: Stability Study of Optimized Formulation (FCNT 10) Over 90 Days.

Storage Condition	Time (Days)	Particle Size (nm)	PDI	Zeta Potential (mV)	Drug Loading Efficiency (%)	Cumulative % Drug Release (24 hr)
(4°C±2°C)	0	255.3±2.8	0.286±0.012	-43.42±1.3	78.5±1.5	67.5±1.5
	30	256.1±2.9	0.289±0.013	-43.1±1.4	78.2±1.6	67.8±1.6
	60	257.0±3.0	0.292±0.014	-42.8±1.4	77.9±1.6	68.2±1.6
	90	258.2±3.1	0.295±0.015	-42.5±1.5	77.4±1.7	68.9±1.7
(25°C±2°C/ 60%±5% RH)	30	262.4±3.2	0.312±0.016	-40.8±1.5	75.6±1.8	72.3±1.8
	60	268.9±3.5	0.335±0.018	-38.5±1.6	73.2±1.9	76.8±2.0
	90	276.5±3.8	0.358±0.020	-35.9±1.7	70.1±2.1	81.4±2.2
(40°C±2°C/ 75%±5% RH)	30	268.2±3.4	0.328±0.017	-39.2±1.6	74.1±1.8	74.5±1.9
	60	279.6±3.9	0.362±0.019	-36.4±1.7	70.5±2.0	79.3±2.1
	90	291.3±4.2	0.394±0.022	-33.2±1.8	66.8±2.2	85.6±2.3





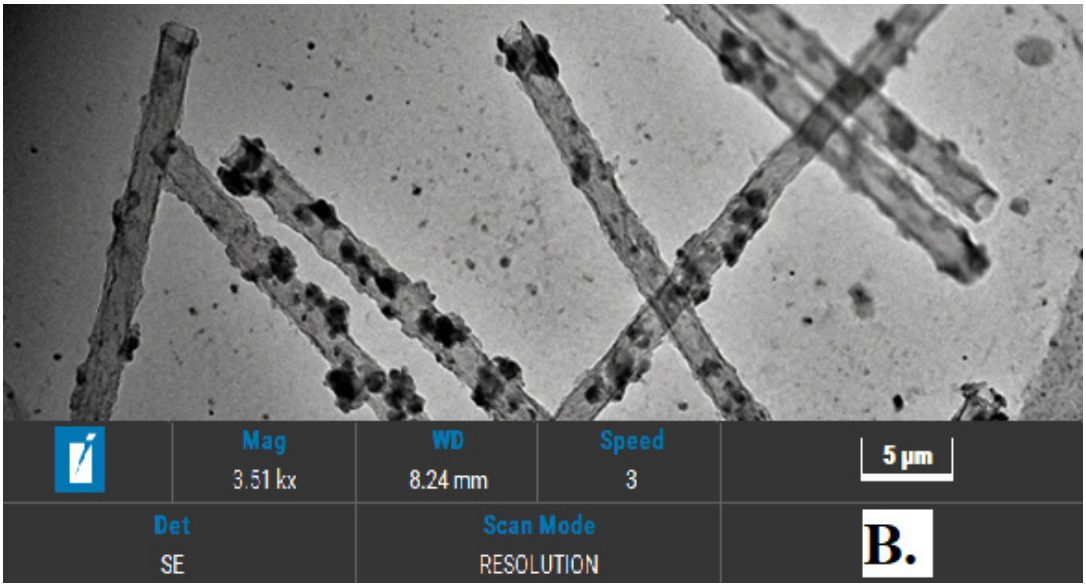


Figure 3: Drug Release Study of the Prepared Batches of Faropenem Loaded MWCNT, and TEM of Placebo MWCNT (A), TEM of Optimized Formulation (B).

release constant (k) and the Korsmeyer-Peppas release exponent (n) as dependent variables and drug:CNT ratio and sonication time as independent variables, revealed a statistically significant overall multivariate effect (Wilks' λ=0.027; $p<0.05$), confirming that these formulation parameters jointly influence the release mechanism.

The Korsmeyer-Peppas release exponent (n=0.544) indicates anomalous non-Fickian transport in cylindrical geometries, as the MWCNT-COOH nanocomposite assumes a cylindrical form confirmed by TEM imaging. For cylindrical systems, n=0.45 indicates Fickian diffusion, while n=0.544 suggests a blend of diffusional release and polymer chain relaxation/swelling. In spherical geometries, the threshold would be n=0.43, but the cylindrical assumption is more suitable due to the morphology of MWCNTs. Thus, the release exponent was interpreted based on this cylindrical model.

Antibacterial Activity

The antibacterial efficacy was assessed using the agar well diffusion assay. Inhibition zones observed for plain CNTs were 9.2 mm against *Staphylococcus aureus* and 8.5 mm against *Escherichia coli*. Modest zones of inhibition were observed for plain CNTs against *Staphylococcus aureus* (9.2 mm) and *Escherichia coli* (8.5 mm). Zones of 18.4 mm (*S. aureus*) and 16.2 mm (*E. coli*) were obtained with pure faropenem. The results can be witnessed in Table 3. The optimized formulation (FCNT10) showed significantly larger zones: 28.6±1.1 mm against *S. aureus* and 24.3±1.0 mm against *E. coli* - a 55% increase against *S. aureus* and 50% against *E. coli* compared to pure faropenem. The greater inhibition zone observed with FCNT10 compared with free faropenem may reflect the combined contribution of the intrinsic antibacterial activity of MWCNT-COOH and altered drug availability/diffusion. Two-way ANOVA revealed a significant main effect of formulation type (F=124.6, $p<0.001$) and bacterial strain (F=18.3, p=0.004), as well as a significant interaction (F=7.8, p=0.019).

Morphology (TEM)

By Transmission Electron Microscopy (TEM), the optimized formulation's surface morphology was measured and the MWCNTs in the formulation were found to be hollow, elongated and free from significant aggregation. Faropenem loading was observed as dark electron dense patches on the sidewalls and open ends of the nanotubes, which is characteristic of surface adsorption. There was no free drug crystal seen. The nanotubes stayed cylindrical with no breaks or damage to the structure. These slightly roughened surfaces with adherent material were observed with the drug loaded CNTs compared to plain CNTs (smooth, clean surfaces), thus indicating effective drug loading. The results can be seen in Figure 3.

Stability Study

Stability studies conducted for 90 days revealed in Table 4 that all parameters remained relatively stable under refrigeration (4°C): the particle size was unchanged from 255.3 nm to 258.2 nm; the PDI remained below 0.3; the zeta potential exceeded -42 mV; the drug loading efficiency decreased by 1.1% and the cumulative release increased by 0.4% from 67.5% to 68.9%, respectively. There were more significant changes at room temperature (25°C): a particle size of 276.5 nm, a PDI of 0.358, a zeta potential of -35.9 mV, a loading efficiency of 70.1% and the release of 81.4%. The formulation degraded significantly with the accelerated conditions (40°C/75%RH) with the particle size increasing to 291.3 nm, PDI rose to 0.394, zeta-potential dropped to -33.2 mV, loading efficiency dropped by 11.7% (to 66.8%) and release increased to 85.6%. Two-way repeated measures ANOVA confirmed a significant effect of storage condition (F=32.7, $p<0.001$), time (F=18.9, p= 0.002), and a significant condition × time interaction (F=9.4, p=0.011).

Optimization Study

The quadratic models displayed strong predictive capabilities, with R^2 values of 0.947, 0.938, and 0.941 for drug loading, particle size, and drug release. Adjusted R^2 values were 0.912, 0.904, and 0.908, while predicted R^2 values were 0.873, 0.865, and 0.871, confirming no overfitting. Adequate precision values exceeded the threshold of 4, and lack-of-fit was non-significant ($p>0.05$), affirming the models' appropriateness. ANOVA indicated significant linear and quadratic terms (model $p<0.001$), with a design matrix condition number below 100, avoiding aliasing. The low coefficient of variation (3.8-4.5%) supported the models' reliability. Model selection was based on the Coefficient of Determination (R^2), adjusted R^2, predicted R^2, significance of the model and individual terms, lack-of-fit assessment, and adequate precision. The model demonstrating statistical significance together with acceptable agreement between adjusted and predicted R^2 was considered appropriate for prediction and optimization.

For Drug Loading Efficiency (%)

For drug loading efficiency, the quadratic polynomial equation derived from CCD regression was:

$$Y_1=78.3 + 4.2A + 3.6B + 2.8C - 1.5AB - 1.2AC - 0.9BC - 2.3A^2 - 1.8B^2 - 1.4C^2$$

R^2=0.947, Adjusted R^2=0.912, Model p-value <0.001.

Where A=CNT concentration (mg, range: 5-15 mg), B=drug:CNT ratio (range: 0.5-1.5), C=sonication time (minutes, range: 5-15 min). The positive linear regression coefficient for A, B and C suggests that the increase of each variable alone leads to an increase in drug loading. The highest influence (+4.2) was found in concentration of CNT. The negative quadratic terms indicate

a levelling off at higher values. The surface saturation effect is confirmed by the negative interaction terms indicating that a high CNT and a high drug ratio do not add up to improve results which can be seen in Figure 4.

For particle size, the equation was:

$$Y_2 = 256.5 - 12.4A - 8.2B - 15.6C + 3.1AB + 2.5AC + 1.8BC + 4.7A^2 + 3.9B^2 + 5.2C^2$$

R^2=0.938, Adjusted R^2=0.904, Model *p*-value <0.001.

All negative linear coefficients indicate that all three variables decrease particle size when they increase. The sonication time had the greatest influence, as seen in -15.6. This indicates its very important function in breaking the aggregates of nanotube. The positive quadratic terms suggest that very high levels would show diminishing returns. The presence of positive interaction coefficients is seen when high CNT is mixed with high ratio, which may be a result of transient re aggregation or due to higher viscosity. These results can be seen in Figure .

For cumulative drug release at 24 hr, the equation was:

$$Y_3 = 68.2 - 5.8A - 4.5B - 7.2C + 1.6AB + 1.2AC + 0.8BC + 3.4A^2 + 2.7B^2 + 4.1C^2$$

R^2=0.941, Adjusted R^2=0.908, Model *p*-value <0.001.

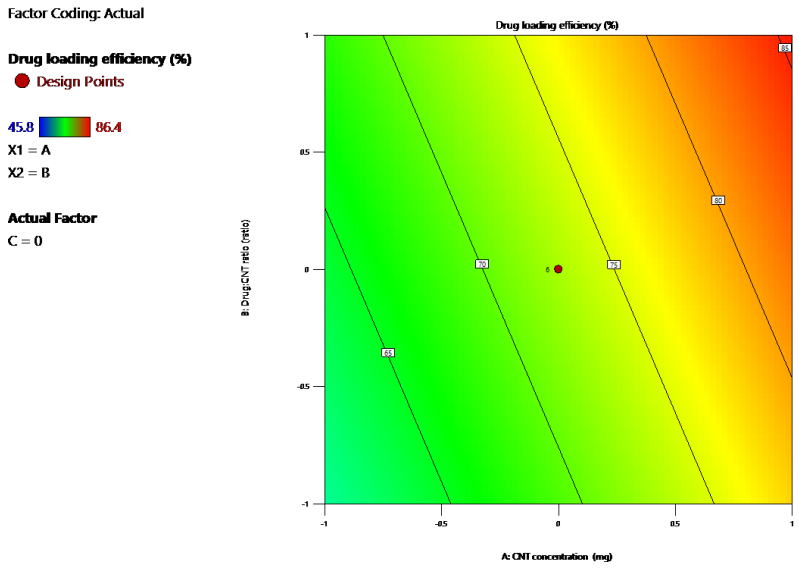
The negative linear coefficients suggest that increasing the concentration of CNT, its drug to CNT ratio and the duration of the sonication, all lead to a reduction in drug release, enhancing the profile to be more sustained. The time of sonication was the factor that had the strongest effect (-7.2). The positive quadratic terms indicate that when release rates are very high, they stay approximately the same or even slightly higher. The optimized batch predicted 67.5% release, which is in agreement with experimental result which can be seen in Figure .

DISCUSSION

The good linearity of the calibration curve of faropenem (R^2=0.999 from 2 to 12 µg/mL) supports the reliability of the UV spectrophotometric method for the quantification of the drug in loading, release and stability studies. This analytical base is the basis for all the following measurements.

The spectroscopic and thermal measurements offer insightful mechanistic understanding of the drug-carrier interaction. The shift in the O-H stretching band with drug loading is indicative of hydrogen bond formation between the hydroxyl/carboxyl groups of faropenem and the hydroxyl/carboxyl groups on the surface of the functionalized nanotubes. Similarly, the small change in the C=O stretching frequency (1760 to 1758 cm^{-1}) suggests weak intermolecular interactions between the β-lactam carbonyl and the electron rich graphene surface of the MWCNTs, probably dipole-dipole or van der Waals forces. These non-covalent interactions are especially desirable for drug delivery systems because they are not strong enough to compromise the integrity of the drug molecule and ensure that it does not leak out prior to reaching its intended target site, yet they are sufficiently weak to allow for easy interaction with the physiological environment (e.g., pH, ionic strength, and competitive binding with serum proteins) and thereby promote the controlled release and desorption of the drug molecule at the target site. Most importantly, no peaks have been observed outside the fingerprint region, and no covalent changes were observed in the core β-lactam ring structure, which is crucial for antibacterial activity, throughout the sonication, lyophilisation and loading procedure. These results collectively prove the chemical compatibility of faropenem with MWCNT-COOH carrier, which validate the formulation strategy adopted in this study.

DSC is in agreement with this: the melting endotherm shifted by about 1°C (from 134.75°C to 133.75°C) and the enthalpy



Factor Coding: Actual

Drug loading efficiency (%)

Design Points

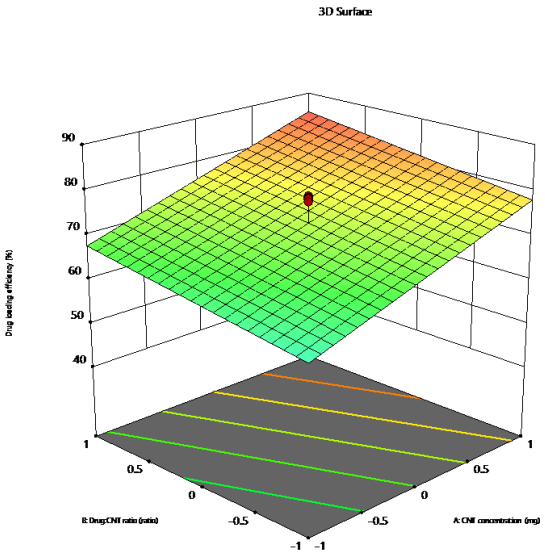
45.8 86.4

X1 = A

X2 = B

Actual Factor

C = 0



Factor Coding: Actual

Particle size (nm)

Design Points

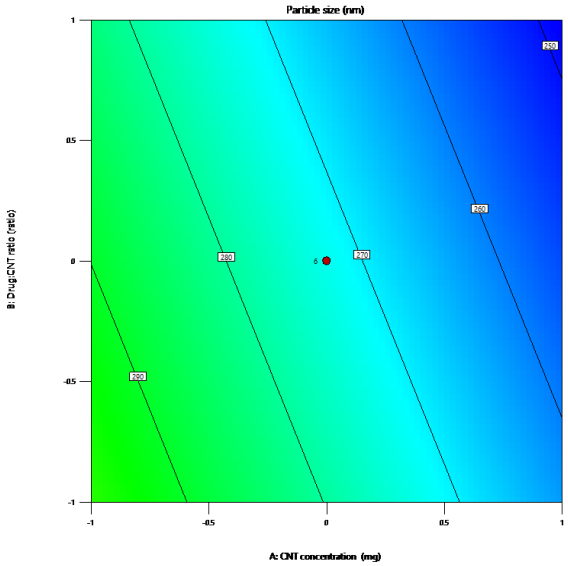
248.9 338.2

X1 = A

X2 = B

Actual Factor

C = 0



Factor Coding: Actual

Particle size (nm)

Design Points

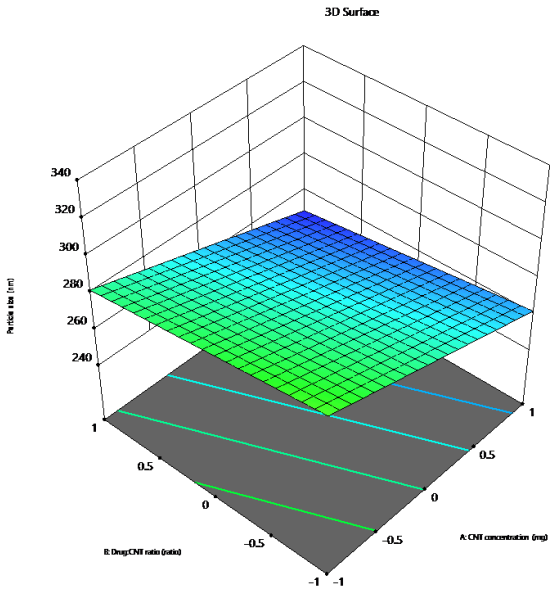
248.9 338.2

X1 = A

X2 = B

Actual Factor

C = 0



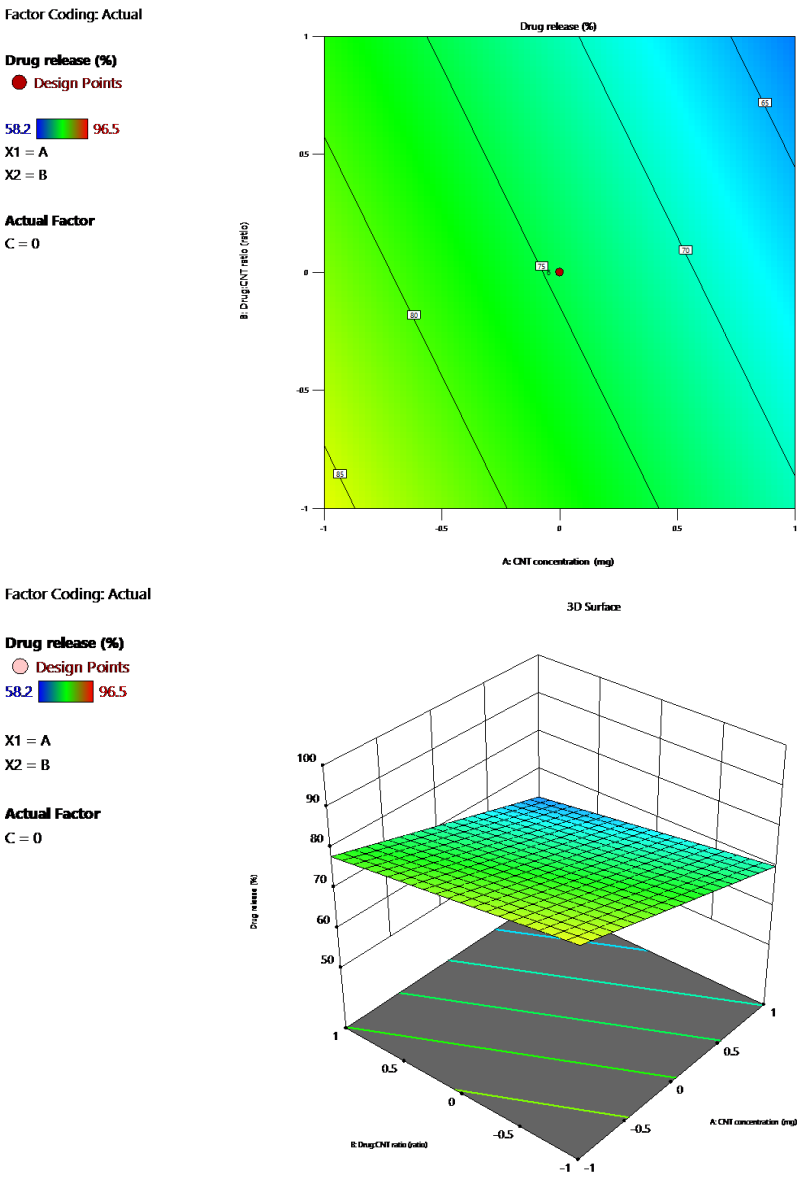


Figure 4: Contour Plots and 3D Plots for Drug Loading Efficiency, % Drug Release (at 24 hr), and Particle Size (nm).

decreased by almost 50% (from ~94 J/g to 46-47 J/g). This means it is partially amorphised and not chemically modified. The second peak around 168.75°C is attributed to the matrix of MWCNT-COOH, which also confirms the composite nature of the formulation.

The crystalline structure of the drug was essentially preserved after loading onto the carbon nanotubes, as confirmed by X-ray diffraction analysis. Small changes in angles and small reductions in maximum intensity were observed, but these changes pointed towards physical adsorption and not chemical degradation. No new diffraction signals were observed to indicate any unwanted polymorphic changes or degradation from products.

The CCD batches showed a wide range of drug loading efficiencies from around 46% to 86%, which was extremely useful for the experimental design, because it allowed the model to distinguish clearly the effect of each formulation variable. Statistical testing revealed that all three independent parameters, CNT concentration, drug to carrier ratio and sonication time, significantly influenced drug entrapment with CNT concentration having the strongest effect.

Specifically, the optimized batch had a loading value in good agreement with the model prediction, confirming the reliability of the quadratic equation. The time of sonication was the most dominant factor in disaggregating the nanotube aggregates for particle size. However, a significant interaction between the sonication time and drug ratio suggested that drug coated nanotubes needed longer sonication time to achieve similar size reduction, possibly due to increased mass or changed surface properties.

An ideal particle diameter of around 255 nm coupled with a low polydispersity index offers a good compromise - small enough to avoid rapid clearance by the reticuloendothelial system but large enough to carry a significant drug payload. Zeta potential measurements revealed a highly negative surface charge for the optimized formulation, significantly above the ±30 mV threshold for colloidal stability. The increased electrostatic repulsion was found to be concentration-dependent of CNTs, which effectively prevents particle aggregation during storage and in the biological milieu. Also, the formulation improved at higher ratios of CNT and drug, their combined effect reduced the loss of drug during centrifugation, leading to satisfactory recovery of about 83%.

The release behaviour was found to be highly tunable ranging from a rapid burst pattern to a distinctly sustained profile depending on the formulation parameters. The optimized system released about 68% of its contents over 24 hr, which offers a promising basis for once daily dosing. The analysis indicates that the Korsmeyer-Peppas model is applicable, with an exponent suggesting a combination of diffusion and carrier relaxation in the release behavior of MWCNTs. The n value of 0.544 reflects both diffusional release and polymer chain effects, though the presence of polydispersity (PDI 0.272-0.478) highlights that the actual release may differ among particle sizes. Smaller particles might release faster due to their higher surface area-to-volume ratios, suggesting the need for future studies to explore particle population dynamics for more precise insights into the release mechanisms.

The most striking finding however was the antibacterial performance. The optimized nanocarrier produced inhibition zones against*S. aureus* about twice the size of those of plain nanotubes and about 50% larger than that of the free drug, with similar significant improvement against*E. coli.* It is important to note that the observed antibacterial activity of the optimized formulation represents the cumulative effect of multiple mechanisms. The plain MWCNT-COOH showed modest intrinsic antibacterial activity (9.2 mm against *S. aureus* and 8.5 mm against *E. coli*), likely attributable to physical membrane disruption, oxidative stress, and the presence of carboxyl functional groups that may interact with bacterial cell surfaces. This intrinsic activity, combined with the sustained release of faropenem from the nanotube surface, contributed to the enhanced zones of inhibition. The high local concentration of drug at bacterial surfaces, improved drug stability within the CNT matrix, and enhanced penetration through cell walls may further amplify the antibacterial effect. The greater efficacy against Gram-positive *S. aureus* compared to Gram-negative *E. coli* suggests that the outer membrane of Gram-negative bacteria may act as a barrier limiting drug accessibility. This combined effect, rather than a simple additive interaction, underscores the potential of functionalized CNTs as delivery systems that can simultaneously exert intrinsic antibacterial activity and provide controlled drug release.

When compared to previously reported antibiotic delivery systems based on CNTs, the drug loading (78.5%) is in the upper range of the reported range for antibiotic delivery systems based on CNTs, and is similar to highly functionalized antibiotic systems based on ciprofloxacin-CNTs. This results in the sustained release over 24 hr with anomalous transport kinetics which is beneficial over the burst release formulations that offer prolonged therapeutic exposure, suitable for once daily administration. Additionally, the high synergy of the antibacterial effect (≈50-55% greater zone diameter) is consistent with reports of improved antimicrobial activity for covalently or strongly adsorbed CNT-antibiotic conjugates relative to free antibiotics and physical mixtures of the two.[32-34]

Transmission electron microscopy confirmed the uniform deposition of faropenem as an amorphous thin layer along the intact sidewalls of the MWCNTs with no evidence of crystalline aggregates or structural damage to the tubular framework. These findings are consistent with the narrow size distribution and low polydispersity index of the formulation. The three-month stability study clearly defined the storage roadmap. All the critical quality attributes (particle size, polydispersity, zeta potential, drug loading and release kinetics) were maintained with negligible fluctuations after refrigeration at 4°C. Ambient temperatures led to significant drug desorption and degradation, while accelerated conditions (40°C/75 % RH) induced considerable particle growth, increased size distribution width and a sharp decrease in drug entrapment. Statistical analysis revealed that storage condition and its interaction with time were highly significant determinants. This implies that refrigerated storage is mandatory for long term use but brief exposure to room temperature may be permissible during transport or patient handling.

To address the well-known biosafety concerns of carbon nanotubes, carboxyl functionalization was used to improve aqueous dispersibility and reduce the intrinsic toxicity of pristine materials. However, the good physicochemical properties, such as a highly negative zeta potential and low PDI, do not diminish the need for direct biological safety evaluations, including cytotoxicity, hemolysis, and *in vivo* toxicological evaluation. The polynomial regression models that were generated were highly predictive and proved that the sonication time had the most significant impact on the decrease of particle size and that all three factors increased the loading efficiency up to a saturation point. Notwithstanding these successes, the antibacterial evaluation was restricted to the agar well diffusion method against two standard strains and thus complementary assays such as minimum inhibitory concentration, time kill kinetics and biofilm disruption studies are needed. Finally, this basic work

opens the way to a robust nanoplatform but requires complete *in vitro* and *in vivo* safety assessment, before clinical translation.

CONCLUSION

Finally, the present research confirmed a statistical method using a Central Composite Design (CCD) to formulate the carboxyl-functionalized multi-walled Carbon Nanotubes (CNTs) loaded with faropenem. The quadratic models were found to have very good predictive power (R^2>0.94), with parameters that achieved an optimum level of drug entrapment (78.5%), an optimum nanometric size (~255 nm), and an excellent level of colloidal stability (zeta potential of −43.4 mV). The optimized nanocarrier exhibited a biphasic sustained release profile comprising non-Fickian transport kinetics that exhibited a reduced initial burst with prolonged release of 24 hr. In addition, this release phenomenon and the antibacterial effect of the CNT matrix pushed the inhibition zones by 50-55% higher than those of the free drug against Gram-positive and Gram-negative pathogens, which may be useful for tackling multidrug resistance. The crystallinity, chemical integrity and the stability of the drugs preserved for 90 days under refrigerated condition indicates their feasibility for long term storage and commercial use. The optimized platform is flexible for use with other labile antimicrobials and offers a scalable, cost-effective approach to enhance patient adherence to reduce dosing frequency. Further *in vivo* pharmacokinetic and biodistribution and toxicological study are needed, as well as an assessment of immunogenicity, but the study is promising. The work done in this study provides a platform for clinical translation of functionalized CNTs as novel adjuvants to combat antimicrobial resistance.

ACKNOWLEDGEMENT

The authors are thankful to the management and Dean/principal of the School of Pharmacy, GH Raisoni University, and Dr. Rajendra Gode Institute of Pharmacy, Amravati for their support which was required for the completion of the project.

ABBREVIATIONS

ANOVA: Analysis of Variance; **CCD:** Central Composite Design; **CNT:** Carbon Nanotube; **DSC:** Differential Scanning Calorimetry; **FTIR:** Fourier Transform Infrared Spectroscopy; **MANOVA:** Multivariate Analysis of Variance; **MWCNT:** Multi-Walled Carbon Nanotube; **PDI:** Polydispersity Index; **TEM:** Transmission Electron Microscopy; **XRD:** X-ray Diffraction.

CONFLICT OF INTEREST

The authors declare that there is no conflict of interest.

ETHICAL APPROVAL

Not Required.

PATIENT CONSENT

Not Required.

AUTHORS CONTRIBUTION

Concept: V.M; **Design:** V.M, S.M; **Supervision:** V.M, S.M, K.N; **Resources:** V.M., K.N; **Materials:** V.M., P.M.; **Acquisition and Handling of Data:** V.M, P.M, K.N; **Analysis and Insights: V.M, S.M; Bibliography Search:** S.M, K.N; **Drafting:** V.M, S.M, K.N, P.M.; **Critical Assessment:** V.M, K.N, S.M.

SUMMARY

In summary, the present study successfully developed and statistically optimized a faropenem-loaded carboxyl-functionalized multi-walled carbon nanotube formulation using a Central Composite Design approach. The optimized formulation demonstrated high drug-loading efficiency, desirable particle characteristics, sustained drug release, and significantly enhanced antibacterial activity compared with free faropenem. Physicochemical characterization confirmed successful drug incorporation without evidence of chemical incompatibility, while stability studies indicated acceptable storage stability under refrigerated conditions.

Although these findings demonstrate the potential of functionalized MWCNTs as promising nanocarriers for controlled antibiotic delivery, additional investigations are necessary before clinical application. Future studies should focus on comprehensive cytotoxicity evaluation, hemocompatibility, pharmacokinetic behaviour, biodistribution, and *in vivo* therapeutic efficacy to establish the long-term safety and translational potential of this delivery platform.

REFERENCES

1. Kalhapure RS, Suleman N, Mocktar C, Seedat N, Govender T. Nanoengineered drug delivery systems for enhancing antibiotic therapy. Journal of pharmaceutical sciences. 2015;104(3):872-905.
2. Ménard-Moyon C, Kostarelos K, Prato M, Bianco A. Functionalized carbon nanotubes for probing and modulating molecular functions. Chem Biol. 2010;17(2):107-15. doi: 10.1016/j.chembiol.2010.01.009.
3. Bianco A, Kostarelos K, Prato M. Applications of carbon nanotubes in drug delivery. Current opinion in chemical biology. 2005;9(6):674-9.
4. Lacerda L, Bianco A, Prato M, Kostarelos K. Carbon nanotubes as nanomedicines: from toxicology to pharmacology. Advanced drug delivery reviews. 2006;58(14):1460-70.
5. Kang S, Herzberg M, Rodrigues DF, Elimelech M. Antibacterial effects of carbon nanotubes: size does matter!. Langmuir. 2008;24(13):6409-13.
6. Gandra S, Takahashi S, Mitrani-Gold FS, Mulgirigama A, Ferrinho DA. A systematic scoping review of faropenem and other oral penems: treatment of Enterobacterales infections, development of resistance and cross-resistance to carbapenems. JAC-Antimicrobial Resistance. 2022;4(6):dlac125.
7. Ishikawa K, Uehara Y, Mori N, Mikami Y, Tokioka S, Kobayashi D, *et al.In vitro* Activity and Clinical Efficacy of Faropenem against Third-Generation Cephalosporin-Resistant*Escherichia coli* and*Klebsiella pneumoniae*. Antimicrob Agents Chemother. 2022;66(6):e0012522. doi: 10.1128/aac.00125-22. Epub 2022 Jun 1. PMID: 35647649.
8. Szpisják-Gulyás N, Al-Tayawi AN, Horváth ZH, László Z, Kertész S, Hodúr CJ. Methods for experimental design, central composite design and the Box-Behnken design, to optimise operational parameters: A review. Acta Alimentaria. 2023;52(4):521-37.
9. Lanone S, Andujar P, Kermanizadeh A, Boczkowski J. Determinants of carbon nanotube toxicity. Advanced drug delivery reviews. 2013;65(15):2063-9.

10. Liu Z, Tabakman S, Welsher K, Dai H. Carbon nanotubes in biology and medicine: *in vitro* and *in vivo* detection, imaging and drug delivery. Nano research. 2009;2(2):85-120.
11. Clare JF. Calibration of UV-vis spectrophotometers for chemical analysis. Accreditation and quality assurance. 2005;10(6):283-8.
12. Pavia DL, Lampman GM, Kriz GS, Vyvyan JR. Introduction to spectroscopy. Belmont, USA. 2001; 13.
13. Giron D. Applications of thermal analysis and coupled techniques in pharmaceutical industry. Journal of thermal analysis and Calorimetry. 2002;68(2):335-57.
14. Sobh RA, Nasr HE, Mohamed WS. Formulation and *in vitro* characterization of anticancer drugs encapsulated chitosan/multi-walled carbon nanotube nanocomposites. Journal of Applied Pharmaceutical Science. 2019;9(8):032-40.
15. Myers RH, Montgomery DC, Anderson-Cook CM. Response surface methodology: process and product optimization using designed experiments. John Wiley & Sons; 2016 Jan 4.
16. Ciofani G, Raffa V. Chemically functionalized carbon nanotubes: emerging vectors for cell therapy. Mini Reviews in Medicinal Chemistry. 2009;9(11):1251-61.
17. Liu Z, Chen K, Davis C, Sherlock S, Cao Q, Chen X, Dai H. Drug delivery with carbon nanotubes for *in vivo* cancer treatment. Cancer research. 2008;68(16):6652-60.
18. Stetefeld J, McKenna SA, Patel TR. Dynamic light scattering: a practical guide and applications in biomedical sciences. Biophysical reviews. 2016;8(4):409-27.
19. Bhattacharjee S. DLS and zeta potential-what they are and what they are not?. Journal of controlled release. 2016 Aug 10;235: 337-51.
20. Honary S, Zahir F. Effect of zeta potential on the properties of nano-drug delivery systems-a review (Part 2). Tropical journal of pharmaceutical research. 2013;12(2):265-73.
21. Rampado R, Peer D. Design of experiments in the optimization of nanoparticle-based drug delivery systems. Journal of controlled release. 2023;358:398-419.
22. Pastorin G, Wu W, Wieckowski S, Briand JP, Kostarelos K, Prato M, Bianco A. Double functionalisation of carbon nanotubes for multimodal drug delivery. Chemical communications. 2006;42(11):1182-4.
23. Wieckowski S, Pastorin G, Benincasa M, Klumpp C, Briand JP, Gennaro R, Prato M, Bianco A. Targeted delivery of amphotericin B to cells by using functionalized carbon nanotubes. Angewandte Chemie. International edition. 2005;44:6358-62.
24. Dash S, Murthy PN, Nath L, Chowdhury P. Kinetic modeling on drug release from controlled drug delivery systems. Acta Pol Pharm. 2010;67(3):217-23.
25. Balouiri M, Sadiki M, Ibnsouda SK. Methods for *in vitro* evaluating antimicrobial activity: A review. Journal of Pharmaceutical Analysis. 2016;6(2):71-9.
26. Perez C. Antibiotic assay by agar-well diffusion method. Acta Biol Med Exp. 1990;15:113-5.
27. Williams DB, Carter CB. Diffraction in TEM. InTransmission Electron Microscopy: A Textbook for Materials Science 2009 (pp. 197-209). Boston, MA: Springer US.
28. Malviya V. Design and characterization of thermosensitive mucoadhesive nasal gel for meclizine hydrochloride: Thermosensitive nasal gel of meclizine HCL. International Journal of Pharmaceutical Sciences and Nanotechnology (IJPSN). 2022;15(1):5782-93.
29. Muthu MS, Feng SS. Pharmaceutical stability aspects of nanomedicines. Nanomedicine. 2009;4(8):857-60.
30. Vyas SP, Khar RK. Targeted & controlled drug delivery: novel carrier systems. CBS publishers & distributors; 2002.
31. Hassani M, Tahghighi A, Rohani M, Hekmati M, Ahmadian M, Ahmadvand H. Robust antibacterial activity of functionalized carbon nanotube-levofloxacine conjugate based on *in vitro* and *in vivo* studies. Scientific Reports. 2022;12(1):10064.
32. Zomorodbakhsh S, Abbasian Y, Naghinejad M, Sheikhpour M. The effects study of isoniazid conjugated multi-wall carbon nanotubes nanofluid on *Mycobacterium tuberculosis*. International journal of nanomedicine. 2020: 5901-9.
33. Metwally NH, Saad GR, Abd El-Wahab EA. Grafting of multiwalled carbon nanotubes with pyrazole derivatives: characterization, antimicrobial activity and molecular docking study. International journal of nanomedicine. 2019: 6645-59.
34. Hadidi N, Mohebbi M. Anti-infective and toxicity properties of carbon based materials: graphene and functionalized carbon nanotubes. Microorganisms. 2022;10(12):2439.

Cite this article: Malviya V, Manekar S, Nichat K, Makode P. Central Composite Design Based Optimization of Faropenem-Loaded Functionalized Carbon Nanotubes for Enhanced Antibacterial Activity. Indian J of Pharmaceutical Education and Research. 2027;61:10.5530/ijper.20270174.